^{18}F-Fallypride PET of Pancreatic Islets: In Vitro and In Vivo Rodent Studies

Adriana Garcia*[1,2], Mohammad Reza Mirbolooki*[1], Cristian Constantinescu[1], Min-Liang Pan[1], Evegueni Sevrioukov[1], Norah Milne[3], Ping H. Wang[2,4], Jonathan Lakey†[5], K. George Chandy†[2], and Jogeshwar Mukherjee†[1,2]

[1]Preclinical Imaging Center, Department of Psychiatry and Human Behavior, University of California Irvine, Irvine, California; [2]Departments of Physiology and Biophysics, University of California Irvine, Irvine, California; [3]Department of Radiological Sciences, University of California Irvine, Irvine, California; [4]Division of Endocrinology, Department of Medicine, University of California Irvine, Irvine, California; and [5]Department of Surgery, University of California Irvine, Irvine, California

Islet cell loss in the pancreas results in diabetes. A noninvasive method that measures islet cell loss and also tracks the fate of transplanted islets would facilitate the development of novel therapeutics and improve the management of diabetes. We describe a novel dopamine D_2/D_3 receptor (D_2/D_3R)–based PET method to study islet cells in the rat pancreas and in islet cell transplantation. **Methods:** ^{18}F-fallypride binding to isolated rat islets and pancreas was evaluated in the absence and presence of the D_2/D_3R inhibitor haloperidol. After intravenous ^{18}F-fallypride (28–37 MBq) administration, normal rats and rats pretreated with haloperidol were imaged in a PET/CT scanner and subsequently studied ex vivo for ^{18}F-fallypride localization in the pancreas. A streptozotocin-treated diabetic rat model was used to study localization of ^{18}F-fallypride in the pancreas, in vitro and ex vivo. Rat islet cells were transplanted into the spleen and visualized using ^{18}F-fallypride PET. **Results:** ^{18}F-fallypride bound to isolated islet cells and pancreatic sections with an endocrine or exocrine selectivity of approximately 4; selectivity was reduced by haloperidol, suggesting that binding was D_2/D_3R-specific. Chemical destruction of islets by streptozotocin decreased ^{18}F-fallypride binding in pancreas by greater than 50%, paralleling the decrease in insulin immunostaining. Uptake of ^{18}F-fallypride in the pancreas was confirmed by radiochromatography and was 0.05% injected dose/cm^3 as measured by PET/CT. The ratio of ^{18}F-fallypride uptake in the pancreas to reference tissue (erector spinae muscle) was 5.5. Rat islets transplanted into the spleen were visualized in vivo by ^{18}F-fallypride and confirmed by immunostaining. The ratio of spleen-transplanted islets to erector spinae muscle was greater than 5, compared with a ratio of 2.8 in untransplanted rats. **Conclusion:** These studies demonstrate the potential utility of ^{18}F-fallypride as a PET agent for islet cells.

Key Words: pancreas; islet cells; ^{18}F-fallypride; PET; diabetes

J Nucl Med 2011; 52:1125–1132
DOI: 10.2967/jnumed.111.088583

Loss of insulin-producing cells in the pancreatic islets, the endocrine component of the pancreas, leads to hyperglycemia and development of type 1 (*1*) or type 2 diabetes mellitus (*2*). Noninvasive imaging approaches to detect and follow the loss of islet cells have been pursued with several radioligands including ^{11}C-acetate, ^{11}C-methionine, ^{18}F-FDG, vesicular monoamine transporter-2 radiotracer ^{11}C-dihydrotetrabenazine, and ^{18}F-FPDTBZ 9-fluoropropyl-(+)dihydrotetrabenazine (*3–5*). The use of ^{18}F-fluorodopa to diagnose infants with congenital hyperinsulinism has been recently reported (*6*). There is clearly a great need for a noninvasive imaging approach to monitor islet cells. Such a method would enable earlier and improved diagnosis and management of insulin-related disorders, especially because the pancreas is not an ideal organ for biopsy (*7*).

In vivo imaging of islet cells in the pancreas has been confounded by their low abundance (only 1%–2% endocrine cells dispersed in the whole pancreas). To detect a change in levels of islet cells, a radiotracer has to overcome issues of nonspecific binding to exocrine pancreatic tissue (*8*). Paradoxically, if the pancreas is clearly visualized on a PET scan, it might suggest excessive nonspecific binding to exocrine tissue (exocrine-confounding problem), whereas a weak PET signal from the pancreas may suggest specific binding to islets but the quantitative measurement of binding may be a challenge (endocrine-confounding problem).

Dopamine D_2 receptor (D_2R) expression has been demonstrated on isolated rodent and human islet cells and β-cell lines (*9*), where it colocalizes with insulin granules. Quinpirole, a D_2R agonist, has been reported to inhibit glucose-dependent insulin secretion. Fallypride, a novel dopamine D_2/D_3R imaging agent labeled with either ^{18}F (110-min half-life) (*10*) or ^{11}C (20-min half-life) (*11*), is suitable to study D_2/D_3R in both the human and the nonhuman brain. Because D_2Rs colocalize with insulin-containing secretory granules in rodent and human islets (*9*), ^{18}F-fallypride-labeled D_2Rs may have the potential as surrogate

Received Jan. 28, 2011; revision accepted Mar. 24, 2011.
For correspondence or reprints contact: Jogesh Mukherjee, 162 Irvine Hall, University of California Irvine, Irvine, CA 92697.
E-mail: mukherjj@uci.edu
*Contributed equally to this work as coauthors.
†Contributed equally to this work as senior authors.

markers for imaging pancreatic islet cells in vitro and in vivo.

Our goal in this study was to evaluate the feasibility of ^{18}F-fallypride PET/CT to visualize endogenous islets in the pancreas and islets transplanted into the spleen. The following sets of studies were performed: isolated rat islet cells were used to demonstrate D_2R-mediated binding of ^{18}F-fallypride in vitro, rat pancreatic sections were used to evaluate ^{18}F-fallypride binding in vitro, in vivo PET/CT of ^{18}F-fallypride in rats was used to evaluate imaging of pancreatic islet cells, and ^{18}F-fallypride methodologies to study rat islet transplantation in vivo were evaluated.

MATERIALS AND METHODS

General Methods

Radioactivity was counted using a Capintec dose calibrator, and low-level counting was done using a well-counter. An Inveon preclinical dedicated PET scanner (Siemens Medical Solutions Inc.), with a resolution of 1.45 mm, was used for the PET studies (*12*). An Inveon preclinical CT scanner (Siemens Medical Solutions Inc.) was used for combined PET/CT experiments. All in vivo and ex vivo images were analyzed using Acquisition Sinogram Image Processing (ASIPro; Siemens Medical Solutions, Inc.), Pixelwise Modeling software (PMOD Technologies), and Inveon Research Workplace software. Slices of the rat pancreas and brain were prepared using the Leica 1850 cryotome. In vitro or ex vivo labeled sections were exposed to phosphor films and read using the Cyclone Phosphor Imaging System (Packard Instruments) and analyzed using Optiquant software. All animal studies were approved by the Institutional Animal Health Care and Use Committee of University of California–Irvine.

Islet Isolation

Islets were isolated from Sprague–Dawley rats using collagenase digestion of the pancreas and density-gradient purification of the islets as previously described (*13*). Isolated islets were stained with dithizone to quantify the yield and to estimate purity. Another aliquot of isolated islets was stained with SYTO Green (Invitrogen)/Ethidium Bromide (Sigma-Aldrich) to quantify viability.

^{18}F-Fallypride Synthesis

The synthesis of ^{18}F-fallypride was performed using previously reported methods (*10*). ^{18}F-fallypride was typically obtained in specific activity greater than 74 MBq/nmol in approximately 370- to 740-MBq batches for imaging studies. The final sterile 0.9% saline solution of ^{18}F-fallypride, pH in the range of 6–7, was dispensed for in vitro and in vivo studies.

Autoradiography

Thin-layer chromatography samples, tissue sections, and freshly isolated islets underwent autoradiography using the Cyclone Plus storage phosphor system. The acquired images were then analyzed with Optiquant software, with which each region of interest was measured in digital light units per square millimeter.

Purified rat islets (50 IEQs) were incubated with 0.185 MBq of ^{18}F-fallypride in the absence or presence of 100 μM haloperidol for 1 h in a 37°C water bath. Exocrine tissue was treated the same as islets. The islets were collected from incubation test tubes onto Whatman filter paper that had been presoaked in 0.1% polyethylenamine using a 24-sample Brandel Cell Harvester and were washed 3 times with cold incubation buffer (*10*). Filters were first exposed to phosphor screens for 30 min, and ^{18}F-fallypride activity was determined by autoradiography. Immediately after autoradiography, filters were placed in the center of the field of view of the Inveon PET scanner and imaged for 30 min.

Induction of Diabetes with Streptozotocin

For chemical destruction of pancreatic β-cells, 8-wk-old male Sprague–Dawley rats (~250 g) were administered streptozotocin at a dose of 80 mg/kg (*14*). Rats were classified as diabetic when nonfasting serum blood glucose levels rose above 350 mg/dL for 3 consecutive days.

PET

Before the start of the imaging study, rats were kept fasting in a quiet place for more than 12 h. In preparation for the scans, the rats were anesthetized with isoflurane and then maintained under anesthesia during the scan (4% induction, 2.5% maintenance). All PET images were acquired with an Inveon preclinical PET scanner. After positioning on the scanner bed, rats were injected with 28–37 MBq of ^{18}F-fallypride via the tail vein. Other rats were injected with haloperidol (0.2 mg/kg) 30 min before ^{18}F-fallypride injections. PET studies typically lasted 1.5–3 h. The images were reconstructed using Fourier rebinning and 2-dimensional filtered backprojection (ramp filter and cutoff at Nyquist frequency), with an image matrix of 128 × 128 × 159, resulting in a pixel size of 0.77 mm and a slice thickness of 0.796 mm. All dynamic images were corrected for radioactive decay. Attenuation and scatter corrections were performed using data from a 10-min transmission scan with a ^{57}Co point source before tracer injection. Reconstructed images were analyzed with ASIPro and PMOD software packages.

CT

The animals were prepared for CT scanning as described for the PET studies. Abdominal images of the rats were obtained with the Inveon CT scanner, with a large-area detector (4,096 × 4,096 pixels, 10 × 10 cm field of view). The CT projections were acquired with the detector-source assembly rotating over 360° and 720 rotation steps. A projection bin factor of 4 was used to increase the signal-to-noise ratio in the images. The CT images were reconstructed using cone-beam reconstruction, with a Shepp filter with cutoff at Nyquist frequency resulting in an image matrix of 480 × 480 × 632 and a voxel size of 0.206 mm. The reconstructed CT images were analyzed using the 3-dimensional Visualization toolbox in the Inveon Research Workplace software. For contrast CT, eXIA 160-XL (Binitio Biomedical Inc.) was administered via the tail vein at a dosage of 0.2–0.4 mL (160 mg of iodine per milliliter). To optimize the spleen contrast, CT images of the abdomen were obtained repeatedly at intervals ranging between 15 min and 2 h after eXIA 160-XL injection (*15*).

Combined PET/CT

The Inveon PET and CT scanners were placed in the docked mode for combined PET/CT experiments. Animals were prepared as described previously and positioned in the CT scanner. Abdominal CT scanning was first performed with or without contrast agent preinjection for 30 min. Immediately after the completion of the CT scan, the animals received a tail vein injection of ^{18}F-fallypride (28–37 MBq) and were imaged in the PET scanner for 120–180 min. The acquired CT images were spatially transformed automatically to match the PET image and were used for attenuation correction of the PET data and identification of animal organs.

Islet Transplantation

After isoflurane anesthesia, an inch-long incision was made laterally and the spleen of the recipient rat was exposed and kept moist with saline-soaked gauze. Islet cells in standard cell culture liquid medium were concentrated in polyethylene-50 tubing with 300*g* centrifugation and transplanted to the front end of the spleen using a 25-μL syringe attached to the polyethylene-50 tubing. The total volume injected to the spleen was less than 20 μL. Coagulation foam was used to prevent bleeding after transplantation. The abdominal wall was sutured with 3-0 silk, the incision was stapled, and the animals were allowed to recover normally.

For in vivo imaging of prelabeled islets in the spleen, isolated rat islets (1,500 IEQs) in 0.2 mL of standard cell culture liquid medium were incubated with ^{18}F-fallypride (0.185 MBq/mL) for 1 h at 37°C before transplantation. Islets were washed 3 times with Hanks Balanced Salt Solution, compressed with centrifugation, and then transplanted into the spleen of an isoflurane-anesthetized rat. As a control, isolated rat splenocytes (6×10^6 cells) were treated similarly and transplanted into the spleen of another rat. The rats were imaged supine for 1.5 h. Sodium ^{18}F fluoride (3.7 MBq) was injected intravenously, and the rats were scanned for an additional 30 min to visualize the skeleton.

To facilitate easier identification and differentiation of the spleen from other abdominal organs in vivo, freshly isolated islets (1,500 IEQs) were first transplanted into the spleen. With the rat supine, the spleen was tethered by 3-0 silk sutures to the abdominal wall. The abdomen was sutured, and the rat was injected with ^{18}F-fallypride through the tail vein and imaged with PET for 2 h under 2.5% isoflurane anesthesia. At the end of the experiment, the spleen was isolated and immunostained for insulin and hematoxylin.

In vivo PET/CT visualization of grafted rat islets in the spleen was performed with the spleen in its normal anatomic position. Islets (6,000 IEQs) were transplanted into the spleen. After a 24-h recovery period, the rat was positioned in the PET/CT scanner and administered the contrast reagent eXIA 160-XL (0.4 mL) via the tail vein. Abdominal CT was first performed for 30 min to delineate the spleen (*15*). The rat was subsequently administered ^{18}F-fallypride (32 MBq) by tail vein injection and then imaged for 2 h in the PET scanner.

Statistical Analysis

Statistical differences between groups were determined using an independent Student *t* test with SPSS statistical software (version 13.0 for Windows). A *P* value of less than 0.05 was considered to be statistically significant in all the in vitro and ex vivo studies.

RESULTS

^{18}F-Fallypride Binding to Isolated Rat Islets In Vitro

For ^{18}F-fallypride binding studies, IEQs were approximately 90% pure and approximately 85% viable (Fig. 1A, inset). D_2R-specific ^{18}F-fallypride binding was determined for each sample by subtracting nonspecific binding (in the presence of haloperidol) from total ^{18}F-fallypride binding ($n = 3$). Figure 1A shows that D_2/D_3R-specific ^{18}F-fallypride binding to islets is approximately 4 times higher than exocrine tissue ($P < 0.05$), suggesting ^{18}F-fallypride binds predominantly to islet cells in the endocrine pancreas. ^{18}F-fallypride activity of isolated islet cells, determined by autoradiography (Fig. 1B) or by 30-min scanning with PET (Fig. 1C), was reduced by haloperidol (67% and 66%, respectively, $P < 0.01$), confirming D_2/D_3R-specific binding.

^{18}F-Fallypride Binding to Rat Pancreas In Vitro

Rat pancreatic sections incubated with ^{18}F-fallypride and quantified by autoradiography showed a significant amount of ^{18}F-fallypride binding (Supplemental Fig. 1; supplemental materials are available online only at http://jnm.snmjournals.org). Pancreatic binding was significantly lower than binding in the striatum (Supplemental Fig. 2). Haloperidol significantly reduced ^{18}F-fallypride binding in the pancreas ($P < 0.05$), confirming D_2R-specific binding (Supplemental Fig. 1). In the brain, the striatum exhibited a high degree of D_2R-specific ^{18}F-fallypride binding (Supplemental Fig. 2, $P < 0.01$), in agreement with previous reports (*10*). The ratio of ^{18}F-fallypride binding in the pancreas of control rats versus haloperidol-treated rats was 2.4, whereas that for the striatum in the brain was 77.

^{18}F-Fallypride Uptake by Rat Pancreas In Vivo

After intravenous administration, uptake of ^{18}F-fallypride was seen in various regions in the abdomen, including the liver, stomach, kidneys, pancreas, and other organs (Fig. 2A). Uptake in the pancreas was approximately 0.05% injected dose/cm^3 and exhibited a slow clearance. Preinjection of haloperidol (0.2 mg/kg) displaced approximately 50% of the ^{18}F-fallypride in the pancreas (Fig. 2B), with a pancreas-to-muscle ratio of 5.5 and 2.95 after haloperidol pretreatment. Ex vivo imaging of the pancreas showed a greater than 50% displacement of ^{18}F-fallypride binding by haloperidol ($P < 0.05$) (Fig. 2C). Thin-layer chromatography of ethyl acetate extracts of pancreas and brain excised from a control rat at 3 h after ^{18}F-fallypride (59 MBq) confirmed the presence of ^{18}F-fallypride and no significant metabolites in pancreatic and brain tissues (Supplemental Fig. 3). Activity in the brain was greater than 95% ^{18}F-fallypride, as seen on thin-layer chromatography, whereas in the pancreas it was greater than 90% ^{18}F-fallypride. Collectively, these data indicate that ^{18}F-fallypride uptake occurs in the pancreas in vivo and binds specifically to D_2/D_3Rs.

^{18}F-Fallypride Studies in Streptozotocin-Induced Diabetic Rat Model

The pancreas of diabetic rats ($n = 3$; average random blood glucose, 534 mg/dL) was harvested 7 d after the onset of hyperglycemia (>350 mg/dL). Age-matched nondiabetic rats ($n = 3$; average random blood glucose, 129 mg/dL) were used as controls. Insulin staining showed a substantial loss of islets (86%) in streptozotocin-treated rats, compared with the healthy rats (Fig. 3A, $P < 0.05$). D_2/D_3R-specific ^{18}F-fallypride binding was reduced (56%) in pancreatic sections of streptozotocin-treated rats (Supplemental Fig. 4, $P < 0.05$), paralleling the loss of insulin staining (Fig. 3A). Dopamine D_2/D_3R-specific ^{18}F-fallypride binding to the striatum (region of highest D_2/D_3R expression) and the cerebellum (region of low D_2/D_3R expression) remained unchanged in streptozotocin-treated and control rats (Supplemental Fig. 5), indicating that selective reduction in ^{18}F-fallypride binding to the pancreas in streptozotocin-treated rats was due to islet destruction. Ex vivo PET of the pancreas of streptozotocin-treated rats, compared with age-matched control rats, showed a decrease (68%) in ^{18}F-fallypride (Fig. 3B, $P < 0.01$), corroborating the in vitro autoradiography data.

Islet Cell Transplantation

The spleen has been used as a site for experimental islet transplantation because of its good vascular supply and portal vein insulin delivery and the potential to avoid complications such as bleeding and portal hypertension associated with traditional transplantation through the portal vein (*16–18*). Three types of experiments were performed to demonstrate that rat islets transplanted into the spleen could be visualized by PET.

In the first transplant experiment, islets were prelabeled with ^{18}F-fallypride for 1 h before transplantation into the spleen and as a control splenocytes were prelabeled and transplanted into the spleen of another rat. The prelabeled transplanted islets were clearly visible in the spleen, and no leakage was noted during in vivo imaging (Fig. 4A). No ^{18}F-fallypride activity was retained in the spleen containing the prelabeled transplanted splenocytes (Fig. 4B). Both studies involved 2 imaging sessions; in the first session, the animal was imaged after ^{18}F-fallypride administration to visualize the transplanted islets, and in the second, after intravenous administration of sodium ^{18}F-fluroide to highlight skeletal tissues and the bladder.

Initial experiments involved only PET, which imposed the difficulty of anatomic localization of the spleen. Therefore, we transplanted islets into the spleen of a rat and then used interventional surgery to move and tether the spleen to the abdominal wall (without damaging its blood supply). After the abdomen was closed, ^{18}F-fallypride was administered for PET abdominal imaging (Fig. 5A). ^{18}F-fallypride activity increased with time in the transplanted spleen, and the ratio of ^{18}F-fallypride uptake in the spleen, compared with the erector spinae muscle, was greater than 12 (Fig. 5B). After the imaging session, insulin immunostaining of the excised spleen confirmed the presence of islet cells (Supplemental Fig. 6).

In the third experiment, PET/CT was used to image grafted islets in the spleen in its normal anatomic position. Islets were transplanted into the spleen, and a day later the spleen was delineated using the eXIA 160 CT contrast agent during a 10-min CT scan (Supplemental Fig. 7) (*15*). The rat was then administered ^{18}F-fallypride (32 MBq) by tail vein injection and imaged for 2 h in the PET scanner (Fig. 6A). Regions of interest on the spleen and erector spinae were drawn on CT images and used to extract mean PET ^{18}F-fallypride activity. Compared with muscle, the spleen showed a significantly higher time-dependent increase in ^{18}F-fallypride activity (Fig. 6B). In a control rat (no islets transplanted), ^{18}F-fallypride activity decreased rapidly in the spleen during the scan period, indicating normal clearance from the circulation (Fig. 6B).

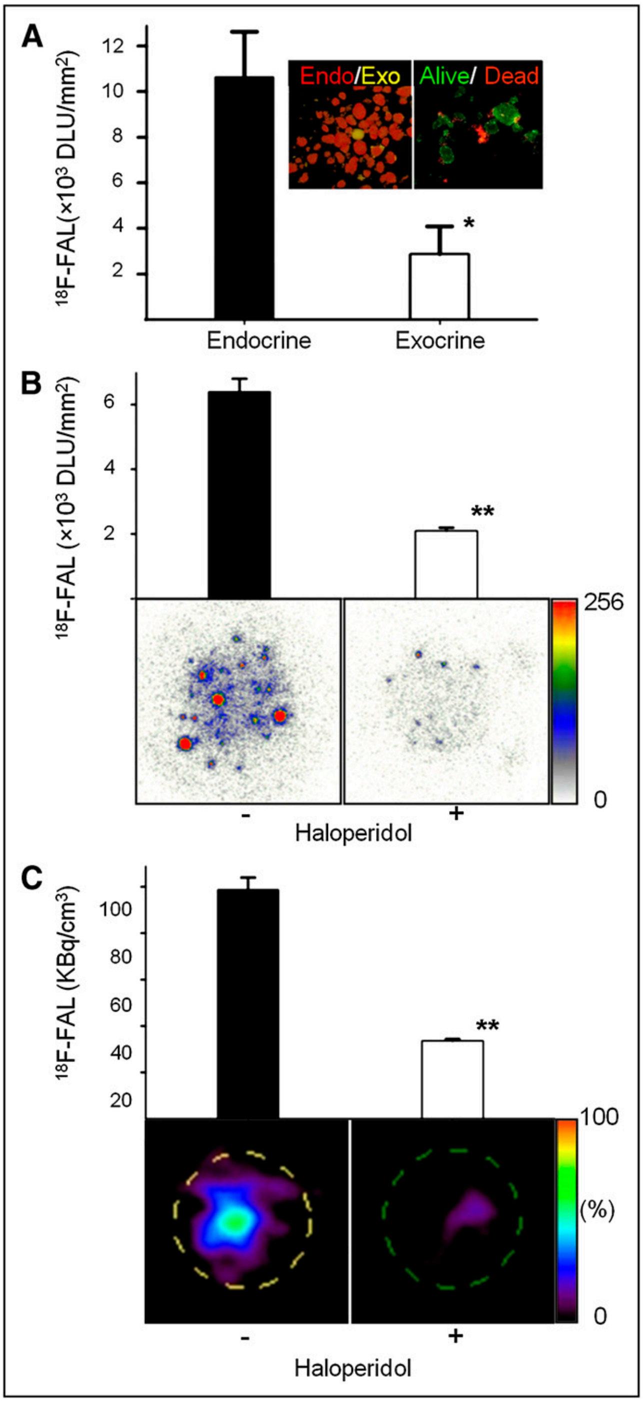

FIGURE 1. ^{18}F-fallypride binding to isolated rat islets. (A) D_2R-specific ^{18}F-fallypride binding to islets and exocrine tissue (n = 3). Inset shows isolated islets stained with the zinc-specific dithizone stain (left) and with SYTO Green/Ethidium Bromide (right). (B) Isolated islets (50 IEQs) labeled with ^{18}F-fallypride in absence or presence of 100 μM haloperidol quantified by autoradiography (n = 5). (C) ^{18}F-fallypride–labeled isolated islets quantified by 30-min PET (n = 5). *$P < 0.05$. **$P < 0.01$. DLU = digital light unit; FAL = fallypride.

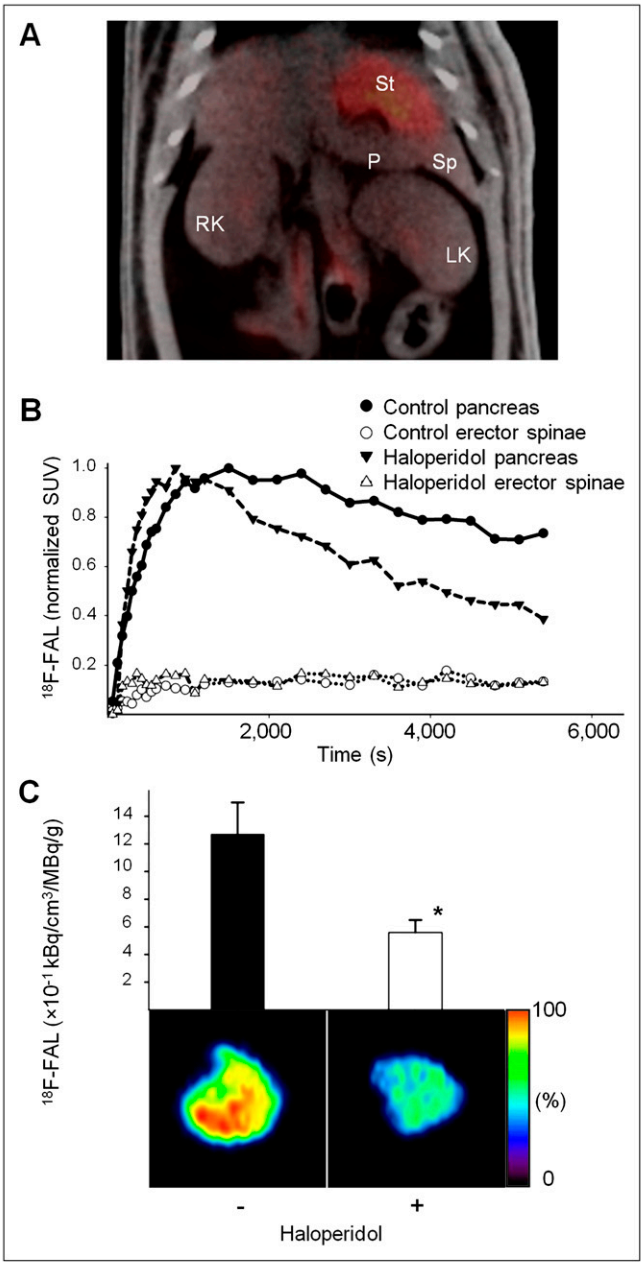

FIGURE 2. (A) PET/CT image of normal rat showing ^{18}F-fallypride uptake at 60–90 min after injection. (B) Normalized uptake in rat pancreas and erector spinae muscle from rats administered ^{18}F-fallypride alone or administered haloperidol (0.2 mg/kg) 1 h before ^{18}F-fallypride. (C) Ex vivo PET of pancreas (n = 3) from rats administered ^{18}F-fallypride with or without administration of haloperidol as in B. Black and white bars indicate ^{18}F-fallypride binding averaged over isolated pancreas (kBq/cm^3) and adjusted by injected dose and tissue weight (n = 3), respectively. FAL = fallypride; LK = left kidney; Pan = pancreas; RK = right kidney; Sp = spleen; St = stomach; SUV = standardized uptake value.

DISCUSSION

Imaging brain dopamine receptors in animal models and human subjects using PET has been successfully performed to understand brain function and pathophysiology (*19*). Imaging of peripheral dopamine receptors has not been pursued as vigorously, primarily because of a continually evolving understanding of their role in other disorders (*20*). The presence of significant levels of dopamine D_2/D_3Rs in the islet cells (*9,21*) and pancreatic tissue (*22*) provided the potential of a surrogate marker to study alterations in insulin secretion. Such a tool could play a significant role in management of diabetes (*3*). Using the dopamine D_2/D_3R PET agent ^{18}F-fallypride, which has been successfully used in brain studies (*23*), we provide strong evidence that ^{18}F-fallypride binds to dopamine receptors in pancreatic islets, suggesting the feasibility of PET/CT with ^{18}F-fallypride to study islet cells.

Pancreatic islets, compared with the hypothalamus in the brain, contain about 3 times as many D_2/D_3Rs (450 fmol/mg vs. 151 fmol/mg of protein) (*22*). Other brain regions containing low concentrations of D_2/D_3Rs, including the hypothalamus, have been successfully imaged using ^{18}F-fallypride (*23,24*). The ability of ^{18}F-fallypride to successfully label D_2/D_3Rs in isolated islet cells over exocrine cells is consistent with greater D_2R immunoreactivity in endocrine tissue (*21*). Residual nondisplaceble binding in islet cells may be associated with other cell types (α and δ). Additionally, the location of dopamine D_2R in the islet cell may affect the ability to remove nonspecifically bound ^{18}F-fallypride (*21*).

Haloperidol inhibition of ^{18}F-fallypride in fresh-frozen pancreas sections was 56%, whereas much higher inhibition was seen in the brain (Table 1). The marked difference between the tissues may in part be due to membrane permeation or accessibility of both ^{18}F-fallypride and haloperidol to the receptor. In brain tissue, dopamine receptors are localized on the readily accessible surface of neuronal cells, whereas in pancreatic tissue, the dopamine receptors are perhaps located both on the membrane surface and internally on insulin secretory granules. Although the competition

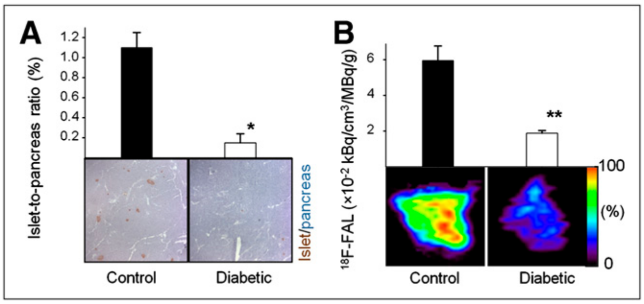

FIGURE 3. (A) Insulin immunostaining of pancreatic sections from normal rats (control) and streptozotocin-treated diabetic rats. Islets are stained brown. Images were quantified using ImageJ software, and ratio of insulin-stained parts (islet) to hematoxylin-stained parts (pancreas) was calculated and expressed as percentage (n = 4). (B) Ex vivo PET of ^{18}F-fallypride activity in pancreas of control and diabetic rats scanned for 30 min. Black and white bars indicate ^{18}F-fallypride binding averaged over isolated pancreas (kBq/cm^3) and adjusted by injected dose and tissue weight, respectively. *$P < 0.01$. **$P < 0.05$. FAL = fallypride.

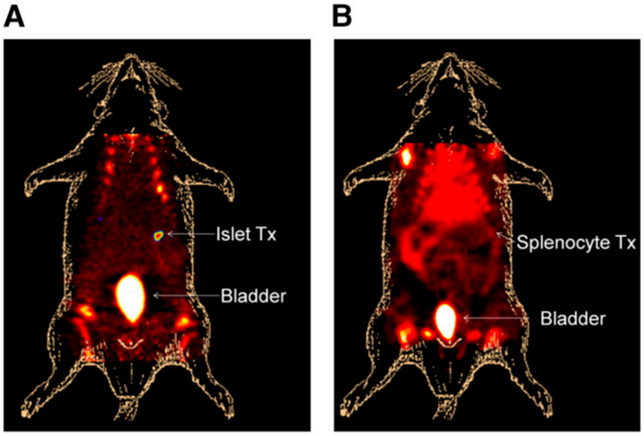

FIGURE 4. (A) In vivo PET visualization of islets prelabeled with ^{18}F-fallypride for 1 h before transplantation into spleen and imaged for 1.5 h after transplantation. After ^{18}F-fallypride scan, ^{18}F-sodium fluoride (3.7 MBq) was injected into rat (to visualize bones and urinary bladder) and imaged for additional 0.5 h. (B) In vivo PET image of ^{18}F-fallypride–prelabeled splenocytes transplanted and imaged in similar fashion to A. FAL = fallypride; Tx = transplantation.

by haloperidol is lower in pancreatic sections, the competition is still significant.

In vivo imaging in rats with ^{18}F-fallypride shows rapid uptake and accumulation in various organs and tissues. Brain uptake is rapid, specific localization in the striatum is approximately 1% of injected dose/cm^3, and binding kinetics in various brain regions have been quantitated (*25*). Compared with the brain, anatomic localization of the pancreas using PET alone has been challenging. Figure 3A shows the use of coregistered PET/CT images of ^{18}F-fallypride to delineate the pancreas. Uptake of ^{18}F-fallypride in the normal pancreas was approximately 0.05% injected dose/cm^3, and is about one twentieth of that found in the striatum. The uptake in the pancreas is similar to the cortical levels in the brain. In haloperidol-pretreated experiments, brain regions exhibit a greater than 90% reduction, whereas pancreatic ^{18}F-fallypride was reduced by approximately 50%. The difference in the degree of displacement of ^{18}F-fallypride in the brain versus pancreas highlights the following issues: differences in the location of the D_2/D_3R slowing clearance of free ^{18}F-fallypride from the pancreas; difference in the tissue content (greater fat content in the pancreas), causing higher nonspecific binding; differences in haloperidol properties (poor membrane permeability), making pancreatic D_2/D_3R less accessible; and a lower component of specific uptake in the pancreas than in the brain.

In streptozotocin-treated diabetic rats, a significant loss of islet cells (>70%–80%) in the pancreas has been reported (*14*). An expected reduction in ^{18}F-fallypride binding to pancreas sections of streptozotocin-treated diabetic rats was observed and paralleled the loss of islets by insulin immunostaining. The extent of ^{18}F-fallypride reduction in the pancreas is consistent with homogenate assays performed using ^{3}H-YM-09151-2 (*22*). Striatal binding of ^{18}F-fallypride in the brain was unaffected; however, previous work on hypothalamus homogenate assays using ^{3}H-YM-09151-2 showed a significant reduction in streptozotocin-treated animals (*22*). The reduction in ^{18}F-fallypride binding in the streptozotocin-treated rats validates the usefulness of this method in a rodent model of type 1 diabetes mellitus.

For in vivo imaging of pancreatic islets, 2 major challenges include the low concentration of endocrine cells and the high nonspecific binding to exocrine cells. Efforts with dihydrotetrabenazine have been uncertain (*5,26*) because of the high nonspecific binding to exocrine cells. Fallypride, which is known to yield higher brain contrast (*23*) than dihydrotetrabenazine (*27*), also exhibits significant nonspecific binding in the pancreas but not as much as dihydrotetrabenazine. Results from this study suggest that approximately 50% of ^{18}F-fallypride in the pancreas may be nonspecifically bound.

Treatment strategies for diabetes include islet cell transplantation (*28*). Significant effort has gone into evaluating the site of transplantation, number of islets, islet survival, islet function, and other factors that determine their efficacy (*29*). Several studies are under way to noninvasively track

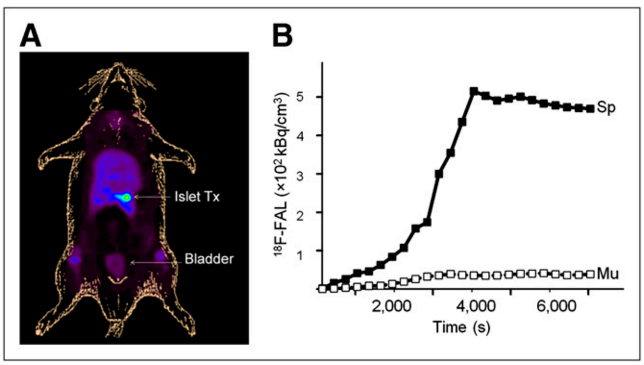

FIGURE 5. (A) In vivo PET visualization of grafted islets in spleen that has been tethered to abdominal wall. ^{18}F-fallypride was administered intravenously. (B) Time–activity curves of ^{18}F-fallypride in transplanted spleen and erector spinae muscle of rat shown in A. FAL = fallypride; Sp = spleen; Mu = erector spinae muscle; Tx = transplantation. Scan lasted 2 h.

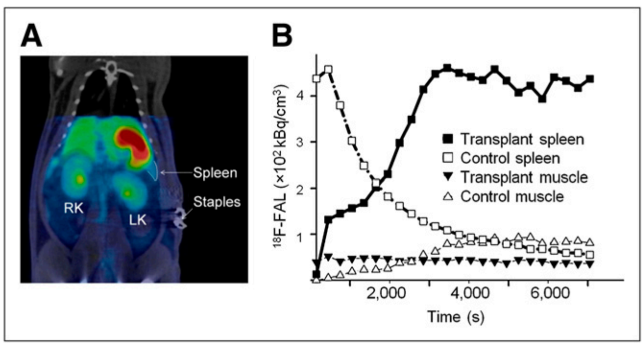

FIGURE 6. (A) In vivo PET/CT visualization of grafted islets in spleen in its normal anatomic position. Spleen was delineated by visualization of eXIA 160-XL contrast agent by CT. (B) Time–activity curves of 2-h ^{18}F-fallypride scan in spleen and erector spinae muscle of control (untransplanted) rat and transplanted rat. FAL = fallypride; LK = left kidney; RK = right kidney.

TABLE 1
^{18}F-Fallypride Binding in Different Organs or Tissues

Study	Islet	Pancreas	Brain
In vitro			
Endocrine vs. exocrine	10.6 ± 1.9 vs. 2.8 ± 1.2; ratio, 3.8*	NA	NA
Control vs. haloperidol	6.4 ± 0.4 vs. 2.1 ± 0.1; ratio, 3.1*	10.6 ± 0.2 vs. 4.4 ± 0.5; ratio, 2.4†	330.1 ± 12.7 vs. 4.3 ± 0.2; ratio, 77†
Control vs. streptozotocin	NA	6.2 ± 0.2 vs. 2.7 ± 0.1; ratio, 2.3‡	38.7 ± 4.9 vs. 44.1 ± 10.1; ratio, 0.9‡
Ex vivo			
Control vs. haloperidol	NA	12.7 ± 2.3 vs. 5.6 ± 0.9; ratio, 2.3§	Ratio, 22‖
Control vs. streptozotocin	NA	5.9 ± 0.8 vs. 1.8 ± 0.1; ratio, 3.3§	NA

*Autoradiography in isolated rat islet cells.
†Autoradiography on tissue slices in absence and presence of haloperidol.
‡Autoradiography on tissue slices in control and streptozotocin-treated animals.
§Small-animal PET on whole isolated pancreas.
‖Small-animal PET on whole isolated brains.
NA = not applicable or not available.
Data are mean ± SD unless otherwise indicated.

transplanted islet cells in vivo. Previous radionuclide studies on islet cell transplantation have included ^{18}F-9-(4-fluoro-3-hydroxymethylbutyl)guanine, which involved imaging modified mouse islets with a recombinant adenovirus expressing herpes simplex virus 1 thymidine kinase (*30*) and glucagon-like peptide 1 receptor radiotracer and imaging autologous human islets transplanted in the left brachioradial muscle using Lys^{40}(Ahx-DTPA-^{111}In)NH_2]exendin-4 (*31*). The latter approach has demonstrated promise. Other imaging modalities continue to be explored for monitoring islet cell transplantation (*32–34*). Our goal in this work was to visualize unmodified transplanted rat islets in vivo. Islet cells prelabeled with ^{18}F-fallypride were visualized after transplantation into the spleen, suggesting retention of receptor-bound ^{18}F-fallypride in vivo. Prelabeled splenocytes transplanted in the spleen did not reveal any selective localization, consistent with lack of dopamine receptors in splenocytes.

Because distribution of ^{18}F-fallypride was prominent in various abdominal organs, eXIA 160-XL CT contrast enabled evaluation of ^{18}F-fallypride in the spleen (Supplemental Fig. 7). In the control rat, the ratio of spleen to erector spinae muscle was 2.8 (Table 2). Uptake in the islet-transplanted spleen was gradual and reached a plateau approximately 50 min after injection of ^{18}F-fallypride (Fig. 6B). The ratio of transplanted spleen to erector spinae muscle was greater than 5. Differences in the ratios in different transplanted animals depended on the number of islets transplanted, the time of imaging after transplantation, and other factors that are currently being investigated.

We have developed a PET/CT method to detect unmodified isolated islets in vivo after transplantation into the spleen. ^{18}F-fallypride is already used in humans to visualize D_2R in the brain. Development of this noninvasive method for clinical trials of islet transplantation is therefore feasi-

TABLE 2
In Vivo Ratios

Parameter	Spleen to muscle	Pancreas to muscle	Striatum to cerebellum
Control	2.83*	5.50†	15‡
Haloperidol treatment	2.03*	2.95†	1.8‡
Islet transplant	12.6§, 5.39‖	NA	NA

*Ratio is normal spleen (without islets) to erector spinae muscle in rats injected with ^{18}F-fallypride intravenously.
†Ratio is pancreas to erector spinae muscle in rats injected with ^{18}F-fallypride intravenously.
‡Ratio in brain dorsal striatum vs. cerebellum at 150 min measured in rats injected with ^{18}F-fallypride intravenously (*25*).
§Ratio is spleen-transplanted islets to erector spinae muscle in rats injected with ^{18}F-fallypride intravenously and spleen moved surgically.
‖Ratio is spleen-transplanted islets to erector spinae muscle in rats injected with ^{18}F-fallypride intravenously.
NA = not applicable or not available.

ble. It may also be possible to use this approach to visualize islets or insulinomas within the pancreas (*21*). The long-term goal of this work is to further evaluate and develop ^{18}F-fallypride as a tracer for monitoring islet cell transplants.

CONCLUSION

The ^{18}F-fallypride method has confirmed the presence of dopamine D_2/D_3Rs in rat islet cells. These receptors are present in significantly larger numbers in the endocrine tissue than in exocrine cells. The islet cells comprise approximately 80% β-cells, which are the insulin-secreting cells. Specific localization of ^{18}F-fallypride and the D_2/D_3R to β-cells remains to be demonstrated. Although ^{18}F-fallypride localizes in vivo in the pancreas, anatomic delineation of the organ is necessary because of low uptake. Paradoxically, because islet cells comprise only 1%–2% of the pancreas, a good endocrine tissue–specific agent in the pancreas may naturally exhibit a low uptake. Approximately 50% of the ^{18}F-fallypride binding seen in the pancreas reflects islet cells. The higher amount of nonspecific binding in the pancreas than in the brain may suggest differences in tissue content and will have to be further evaluated. Transplanted islet cells can be imaged in vivo using ^{18}F-fallypride, and future studies will evaluate clinically relevant islet transplantation sites.

DISCLOSURE STATEMENT

The costs of publication of this article were defrayed in part by the payment of page charges. Therefore, and solely to indicate this fact, this article is hereby marked "advertisement" in accordance with 18 USC section 1734.

ACKNOWLEDGMENTS

We thank Robert Coleman and Ritu Kant for technical assistance and Drs. Sonia Grewal and David Hoyt for discussions. This study was supported by NIH RC1DK087352, NIH F31DK083203, NIH RO1 NS-48252, NIH R01HL096987, JDRF 5-2007-662, the UC Irvine Diabetes Center, and the Department of Surgery. Presentations of this work were given the Berson-Yalow Award 2009 and NIH-JDRF Award 2009. No other potential conflict of interest relevant to this article was reported.

REFERENCES

1. Akirav E, Kushner JA, Herold KC. Beta-cell mass and type 1 diabetes. *Diabetes.* 2008;57:2883–2888.
2. Wajchenberg BL. Clinical approaches to preserve beta-cell function in diabetes. *Adv Exp Med Biol.* 2010;654:515–535.
3. Wu Z, Kandeel F. Radionuclide probes for molecular imaging of pancreatic beta-cells. *Adv Drug Deliv Rev.* 2010;62:1125–1138.
4. Souza F, Simpson N, Raffo A, et al. Longitudinal noninvasive PET-based beta cell mass estimates in a spontaneous diabetes rat model. *J Clin Invest.* 2006; 116:1506–1513.
5. Singhal T, Ding YS, Weinzimmer D, et al. Pancreatic beta cell mass PET imaging and quantification with 11C-DTBZ and 18F-FP-(+)-DTBZ in rodent models of diabetes. *Mol Imag Biol.* September 8, 2010 [Epub ahead of print].
6. Hardy OT, Hernandez-Pampaloni M, Saffer JR, et al. Diagnosis and localization of focal congenital hyperinsulinism by ^{18}F-fluorodopa PET scan. *J Pediatr.* 2007;150:140–145.
7. Sperling MA. PET scanning for infants with HHI: a small step for affected infants, a giant leap for the field. *J Pediatr.* 2007;150:122–124.
8. Sweet IR, Cook DL, Lernmark A, et al. Systemic screening of potential b-cell imaging agents. *Biochem Biophys Res Commun.* 2004;314:976–983.
9. Rubí B, Ljubicic S, Pournourmohammadi S, et al. Dopamine D2-like receptors are expressed in pancreatic beta cells and mediate inhibition of insulin secretion. *J Biol Chem.* 2005;280:36824–36832.
10. Mukherjee J, Yang ZY, Das MK, Brown T. Fluorinated benzamide neuroleptics: III. Development of (*S*)-*N*-[(1-allyl-2-pyrrolidinyl)methyl]-5-(3-[^{18}F]fluoropropyl)-2, 3-dimethoxybenzamide as an improved dopamine D-2 receptor tracer. *Nucl Med Biol.* 1995;22:283–296.
11. Mukherjee J, Shi B, Christian BT, Chattopadhyay S, Narayanan TK. ^{11}C-fallypride: radiosynthesis and preliminary evaluation of novel dopamine D2/D3 receptor PET radiotracer in nonhuman primate brain. *Bioorg Med Chem.* 2004;12:95–102.
12. Constantinescu C, Mukherjee J. Performance evaluation of an Inveon PET preclinical scanner. *Phys Med Biol.* 2009;54:2885–2899.
13. Cheng Y, Zhang JL, Liu YF, Li TM, Zhao N. Islet transplantation for diabetic rats through the spleen. *Hepatobiliary Pancreat Dis Int.* 2005;4:203–206.
14. Islam MS, Loots du T. Experimental rodent models of type 2 diabetes: a review. *Methods Find Exp Clin Pharmacol.* 2009;31:249–261.
15. Willekens I, Lahoutte T, Buls N, et al. Time course of contrast enhancement in spleen and liver with Exia 160, Fenestra LC, and VC. *Mol Imaging Biol.* 2009; 11:128–135.
16. Rajab A. Islet transplantation: alternative sites. *Curr Diab Rep.* 2010;10:332–337.
17. Kaufman DB, Morel P, Field MJ, et al. Purified canine islet autografts: functional outcome as influenced by islet number and implantation site. *Transplantation.* 1990;50:385–391.
18. Aoki T, Hui H, Umehara Y, et al. Intrasplenic transplantation of encapsulated genetically engineered mouse insulinoma cells reverses streptozotocin-induced diabetes in rats. *Cell Transplant.* 2005;14:411–421.
19. Van Laere K, Varrone A, Booij J, et al. EANM procedure guidelines for brain transmission SPECT/PET using dopamine D2 receptor ligands, version 2. *Eur J Nucl Med Mol Imaging.* 2010;37:434–442.
20. Garcia-Tornadu I, Perez-Millan MI, Recouvreux V, et al. New insights into the endocrine and metabolic roles of dopamine D2 receptors gained from the Drd2−/− mouse. *Neuroendocrinology.* 2010;92:207–214.
21. Grossrubatscher E, Veronese S, Dalino P, et al. High expression of dopamine receptor subtype 2 in a large series of neuroendocrine tumors. *Cancer Biol Ther.* 2008;7:1970–1978.
22. Shankar E, Santosh KT, Paulose CS. Dopaminergic regulation of glucose-induced insulin secretion through dopamine D2 receptors in the pancreatic islets in vitro. *IUBMB Life.* 2006;58:157–163.
23. Mukherjee J, Christian BT, Dunigan KA, et al. Brain imaging of ^{18}F-fallypride in normal volunteers: blood analysis, distribution, test-retest studies, and preliminary assessment of sensitivity to aging effects on dopamine D-2/D-3 receptors. *Synapse.* 2002;46:170–188.
24. Mukherjee J, Yang ZY, Brown T, et al. Preliminary assessment of extrastriatal dopamine D-2 receptor binding in the rodent and non-human primate brains using the high affinity radioligand, [F-18]fallypride. *Nucl Med Biol.* 1999;26:519–527.
25. Constantinescu C, Coleman RA, Pan ML, Mukherjee J. Striatal and extrastriatal microPET imaging of D2/D3 dopamine receptors in rat brain with ^{18}F-fallypride and ^{18}F-desmethoxyfallypride. *Synapse.* 2011;65:778–787.
26. Fagerholm V, Mikkola KK, Ishizu T, et al. Assessment of islet specificity of dihydrotetrabenazine radiotracer binding in rat pancreas and human pancreas. *J Nucl Med.* 2010;51:1439–1446.
27. Chan GLY, Holden JE, Stoessl AJ, et al. Reproducibility studies with ^{11}C-DTBZ, a monoamine vescicular transporter inhibitor in healthy human subjects. *J Nucl Med.* 1999;40:283–289.
28. Shapiro AMJ, Ricordi C, Hering BJ, et al. International trial of the Edmonton protocol for islet transplantation. *N Engl J Med.* 2006;355:1318–1330.
29. Medarova Z, Vallabhajosyula P, Tena A, et al. In vivo imaging of autologous islet grafts in the liver and under the kidney capsule in non-human primates. *Transplantation.* 2009;87:1659–1666.
30. Kim SJ, Doudet DJ, Studenov AR, et al. Quantitative micro positron emission tomography (PET) imaging for the in vivo determination of pancreatic islet graft survival. *Nat Med.* 2006;12:1423–1428.
31. Pattou F, Kerr-Conte J, Wild D. GLP-1 receptor scanning for imaging of human beta cells transplanted in muscle. *N Engl J Med.* 2010;363:1289–1290.
32. Low G, Hussein N, Owen RJ, et al. Role of imaging in clinical islet transplantation. *Radiographics.* 2010;30:353–366.
33. Medarova Z, Evgenov NV, Dai G, Bonner-Weir S, Moore A. In vivo multimodal imaging of transplanted pancreatic islets. *Nat Protoc.* 2006;1:429–435.
34. Eriksson O, Eich T, Sundin A, et al. Positron emission tomography in clinical islettransplantation. *Am J Transplant.* 2009;9:2816–2824.